



**HAL**  
open science

# Unsteady flow rate simulations methodology for identification of the dynamic transfer function of a cavitating venturi

Artem Marie-Magdeleine, Regiane Fortes Patella, Nicolas Lemoine, Nicolas Marchand

## ► To cite this version:

Artem Marie-Magdeleine, Regiane Fortes Patella, Nicolas Lemoine, Nicolas Marchand. Unsteady flow rate simulations methodology for identification of the dynamic transfer function of a cavitating venturi. CAV 2012 Symposium, 2012, Singapour, Singapore. 10.3850/978-981-07-2826-7\_020 . hal-02510568

**HAL Id: hal-02510568**

**<https://hal.science/hal-02510568>**

Submitted on 13 Aug 2020

**HAL** is a multi-disciplinary open access archive for the deposit and dissemination of scientific research documents, whether they are published or not. The documents may come from teaching and research institutions in France or abroad, or from public or private research centers.

L'archive ouverte pluridisciplinaire **HAL**, est destinée au dépôt et à la diffusion de documents scientifiques de niveau recherche, publiés ou non, émanant des établissements d'enseignement et de recherche français ou étrangers, des laboratoires publics ou privés.

# Unsteady flow rate evaluation methodology for identification of the dynamic transfer function of a cavitating Venturi.

**Artem MARIE-MAGDELEINE**  
CNES, Evry, France

**Regiane FORTES-PATELLA**  
LEGI, Grenoble, France

**Nicolas LEMOINE**  
Snecma, Vernon, France

**Nicolas MARCHAND**  
GIPSA, Grenoble, France

## SUMMARY

The development of new rocket turbopumps makes it necessary to study different phenomena occurring during cavitation, such as auto-oscillations that can cause the POGO effect and damage the rocket structure if they occur at the structural eigenfrequency. This is why an experimental facility is currently being developed in the Cremhyg laboratory in Grenoble, France in order to perform dynamic characterization of different cavitating devices to define the general identification methodology. The work presented in this paper serves the purpose to test this methodology on a simulation case of the cavitating Venturi computed with the IZ code. The principle of the IZ code is presented in the second paragraph. The first step of the methodology consists of evaluating pressures and mass flow rates at the inlet and the outlet of the cavitating profile and the next steps aims at estimating the dynamic transfer function of the cavitating Venturi. For this purpose, the Kinetic Differential Pressure method was chosen and introduced and its robustness towards evaluation uncertainties is evaluated in the third paragraph. Next, the numerical simulation with the IZ code gives the empirical transfer function results from the precise inlet and outlet pressure data which is later compared with the transfer matrix coefficients obtained with the Kinetic Differential Pressure method using the standard identification procedures such as the Empirical transfer function evaluation and the user-made Auto-Regressive Moving Average exogenous algorithm.

## INTRODUCTION

During the development of a new liquid propellant rocket engine the knowledge of dynamic transfer functions of cavitating turbopumps is primordial in order to correctly assess the risk of POGO phenomenon occurrence and to possibly propose a corresponding solution of an anti-POGO correction. Several studies on this topic were carried by every major space agencies [1-4]. In France, CNES (Centre national d'Etudes Spatiales) and Snecma are currently working in partnership with LEGI, Gipsa-lab and CremHyg laboratories in Grenoble on building a hydrodynamic test facility to perform

identification of transfer functions of different cavitating devices. In order to ensure that the tests go properly, several methods of unsteady flow rate evaluation and signal processing need to be considered. [5-6].

This facility includes devices allowing pressure and flow rate fluctuations in the domain from 5 to 50Hz as well as instrumentation capable of measuring these fluctuations. Different optical (LDV, PIV, PDI, LIF), acoustic (ADV), electromagnetic, thermoanemometric (hot film, hot wire), magnetic resonance and ionization methods were considered [6, 8-12]. Finally, the method using Kinetic Differential Pressures (KDP) [13] was chosen as both the simplest to implement and enough accurate. The performance of this method is presented in this article. This method allows deducing flow rate fluctuations from the unsteady pressure evaluations and thus to obtain all the information the operator needs to identify the dynamic transfer matrix of a cavitating device [3]:

$$\begin{pmatrix} \tilde{P}_s \\ \tilde{Q}_s \end{pmatrix} = \begin{pmatrix} Z_m & Z_L \\ Z_C & Z_M \end{pmatrix} \begin{pmatrix} \tilde{P}_e \\ \tilde{Q}_e \end{pmatrix}$$

All variables are taken in the Fourier frequency domain. The superscript  $\sim$  means that fluctuating quantities are taken, but it will be omitted for the remaining frequency-domain formulae. Before applying KDP method for experimental data processing, a numerical method was developed in order to test and to evaluate the methodology of the mass flow rate restitution and of the dynamic transfer matrix identification. This article describes this methodology and presents its first application results.

## OBJECT OF STUDY

The unsteady flow reconstitution simulation and the system identification algorithms will be tested on the cavitating Venturi CFD computations performed by the 2D unsteady code "IZ", which has been developed in our team with the support of the CNES-Centre National d'Etudes Spatiales. The code solves the Reynolds Averaged Navier-Stokes equations for a homogeneous fluid; it applies the k- $\epsilon$  RNG turbulence model associated to a barotropic approach to the cavitation modeling. The numerical code is widely described in [7], and has been

previously validated under different cavitating flow configurations.

The studied Venturi (Fig.1) is coupled to the pipes at the inlet and the outlet of the system (Fig.2). The circuit impedance is modeled by a 1D hydro-elastic model that solves the Allievi's equations.

$$\frac{\partial p}{\partial t} + u \frac{\partial p}{\partial x} + \rho a^2 \frac{\partial u}{\partial x} = 0 \quad \frac{\partial u}{\partial t} + u \frac{\partial u}{\partial x} + \frac{1}{\rho} \frac{\partial p}{\partial x} + C_f \frac{|u|}{2D} = 0$$

where  $u$  is the speed of the fluid flow,  $p$  is the pressure,  $C_f$  is the friction factor,  $D$  the pipe diameter,  $\rho$  the water density,  $x$  the coordinate and  $a$  the sound speed in the pipe, which is defined from the sound speed in the water, pipe wall thickness  $e$  and Young modulus  $E$ :

$$a = \frac{c}{\sqrt{1 + \frac{\rho_{water} c^2 D}{e E}}}$$

These equations are solved by using the Method of Characteristics MOC. Head losses are modelled by the diaphragm approach [19].

The different boundary conditions during this study are the total reflection (pressure node) or the total absorption at the outlet (no-reflecting boundary conditions [18]). The mass flow is imposed at the inlet. This choice is a primordial part of the system identification procedure. Typically the imposed flow rate fluctuations are either a sum of several sinusoids or a chirp signal. Depending on the inlet excitation signal, different data post-treatment algorithms may be applied in order to determine the dynamic transfer matrix terms.

Calculations presented in this paper concern cold water, a mean flow rate equal to 15.5L/s and inlet mean sigma coefficient value of about 2.4. The fluctuating pressure and flow rates are taken by 3 pressure sensors placed in the inlet pipe and 3 in the outlet pipe equidistantly (Fig. 2).

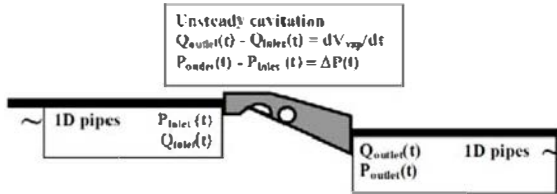


Figure 1: Venturi pipe coupling

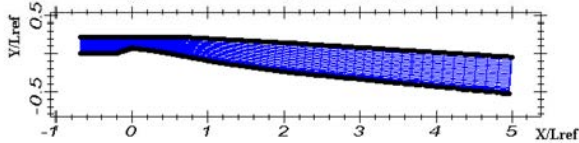


Figure 2: Venturi geometry

### KDP BACKGROUND THEORY

In this part equations characterizing the KDP method are described. They are applied in the case of a simple duct in order to evaluate the accuracy and the robustness of the method when sensor data is polluted with a noise term.

### General equations

Three equidistant points at the inlet pipe and three nodes at the outlet one are chosen as the positions of the pressure sensors. The pressure data at these nodes is used to estimate the unsteady flow rate in the pipe using the acoustic wave equations. The pressure signal is composed of one wave travelling in one direction and another wave travelling in the opposite direction [5, 6, 13]:

$$p(x, \omega, t) = \rho g (A e^{i\omega(t - \frac{x}{a})} + B e^{i\omega(t + \frac{x}{a})})$$

Let  $k = \frac{2\pi f}{a}$ . Hence the values read on the pressure sensors can be written the following way after a Fourier transform, and the system of equations is solved in order to obtain the values of ascending and descending waves  $A$  and  $B$  and for the sound speed  $a$ :

$$\begin{aligned} P_1(f) &= \rho g (A(f) e^{ikt} + B(f) e^{-ikt}) \\ P_2(f) &= \rho g (A(f) + B(f)) \\ P_3(f) &= \rho g (A(f) e^{-ikt} + B(f) e^{ikt}) \\ \frac{P_1 + P_3}{2P_2} &= \frac{e^{ikt} + e^{-ikt}}{2} = \cos\left(\frac{2\pi f l}{a}\right) \\ a &= \frac{2\pi f l}{\arccos\left(\left\|\frac{P_1 + P_3}{2P_2}\right\|\right)} \end{aligned}$$

The value of the sound speed  $a$  is to be taken at the frequency  $f$  where the signal spectral density is important to be more precise. The expressions of the unsteady pressure and the unsteady mass flow rate at every coordinate  $x$  of the pipe can be estimated using these acoustic wave equations:

$$\begin{aligned} P(x, f) &= \rho g (A(f) e^{-ikx} + B(f) e^{ikx}) \\ Q(x, f) &= \frac{\rho g S}{a} (A(f) e^{-ikx} - B(f) e^{ikx}) \end{aligned}$$

It seems important to notice that the values of  $P$  and  $Q$  could be taken elsewhere from the measuring sections; hence the KDP method can also be used to extrapolate the unsteady pressure and mass flow rate data closer to the inlet and the outlet of the cavitating device to be characterized.

In order to reconstruct time-domain data of the unsteady flow rate an inverse Fourier transform may be taken. However, for the identification purposes only the frequency domain data taken at the modulation frequency is needed. Firstly, several calculations have been performed on a 1D line. At one end of the line the flow rate was modulated by a user as a sum of sine waves or as a chirp signal, and on the other end of the hydraulic line a totally reflecting limit condition was implemented. The CFL condition was set to be equal to 1. The test section had a length of 12 m split into 41 nodes separated by 30cm, the initial sound speed was 928m/s, and thus the time step  $dt$  was  $3.2 \cdot 10^{-4}$  s which is  $0.01 T_{ref}$ . The position of the points giving the pressure information  $P_1$ ,  $P_2$ ,  $P_3$  are typically the 5<sup>th</sup>, 20<sup>th</sup> and 35<sup>th</sup>. However, the acoustic wave equations allow extrapolating the values of pressures and mass flow rates closer to the duct boundaries, i.e. at the 1<sup>st</sup> and the 41<sup>st</sup> nodes. The results of the sound speed estimation and the flow rate reconstruction from the pressure nodes data showed to be in a good agreement with the originally implemented values. For the sound speed, typical estimation errors were about 1% and for the flow rate the amplitude of a reconstructed signal may present the difference up to 3% with the simulated signal. The comparison between the original simulated flow rate and the reconstructed values are given at the Fig. 3 and 4:

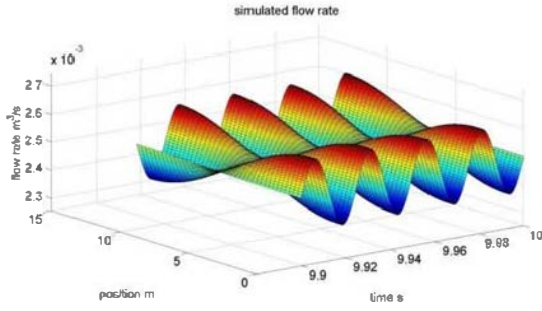


Figure 3: Simulated flow rate

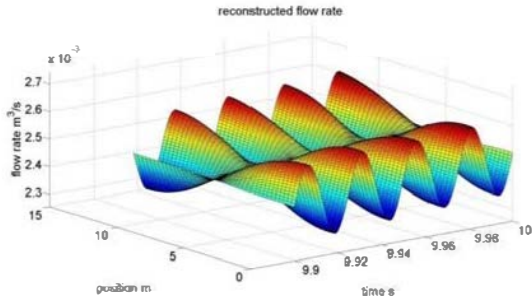


Figure 4: Reconstructed flow rate

The small differences between the two surfaces may be explained by the head losses taken into account for the simulation ( $\lambda=0.019$ ) but not taken into account in the acoustic wave equation used for mass flow rate reconstitution. The Root Mean Square error is about 10% between the frequency domain signals of the simulated and the reconstructed flow rates.

#### Transfer matrix evaluation method

Once the inlet and outlet pressure and mass flow rate frequency domain data is obtained, it is possible to evaluate the coefficients of the transfer matrix. As there are in all 2 inlet and 2 outlet variables, it is necessary to perform a series of tests with the linearly independent inlet frequency-domain data vectors ( $P_{e1}, Q_{e1}$ ) and ( $P_{e2}, Q_{e2}$ ). This can be achieved through different procedures. Firstly, the inlet mass flow rate amplitude variation fixed by the user does not imply inlet pressure fluctuations to vary proportionally. The other way to proceed is to change the pipeline boundary conditions, that is for instance to test the pressure node condition totally reflecting acoustic waves and the “free outlet” condition without any reflection. Moreover, the system linearity can be tested with at least 3 non-collinear input data vectors ( $P_{ei}, Q_{ei}$ ). The expressions of the transfer matrix coefficients are the following:

$$Z_m = \begin{bmatrix} P_{s1} & Q_{e1} \\ P_{s2} & Q_{e2} \\ P_{e1} & Q_{e1} \\ P_{e2} & Q_{e2} \\ Q_{s1} & Q_{e1} \\ Q_{s2} & Q_{e2} \end{bmatrix} \quad Z_l = \begin{bmatrix} P_{e1} & P_{s1} \\ P_{e2} & P_{s2} \\ P_{e1} & Q_{e1} \\ P_{e2} & Q_{e2} \\ P_{e1} & \epsilon_{e1} \\ P_{e2} & \epsilon_{e2} \end{bmatrix} \quad Z_c = \begin{bmatrix} P_{e1} & Q_{e1} \\ P_{e2} & Q_{e2} \end{bmatrix} \quad Z_u = \begin{bmatrix} P_{e1} & Q_{e1} \\ P_{e2} & Q_{e2} \end{bmatrix}$$

This evaluation method is called the Empirical Transfer Function Evaluation, or ETFE. It gives satisfactory results if the signal to noise ratio is high enough. Otherwise, other methods may be used, e.g. auto-recursive methods such as ARMAX [14, 15], which will be presented later in the article.

#### KDP Method robustness evaluation

The pressure sensors used may present high uncertainty values. The possible evaluation errors may come from internal causes

(sensor calibration, numerical noise, linearization errors, and pipe vibrations) as well as from external ones (electromagnetic pollution from neighboring facilities) [16]. This is why it is important to test the algorithm robustness in case when the signal to noise ratio is low.

To this extent, a random Gaussian noise variable is added to the simulated pressure signal, uncertainty propagation is studied and the obtained results are compared with those corresponding to the ‘clean’ simulation.

#### Propagation from $P(t)$ to $P(j\omega)$

The error on the time-domain signal is noted  $\eta(t)$  and the one on the frequency-domain signal is  $\epsilon(j\omega)$ . The time-domain error is a Gaussian zero-centered white noise uncorrelated with  $P(t)$ , and its amplitude may be estimated if the operator knows the possible error causes. The values of time-domain and frequency-domain errors are linked by the Parseval Formula for the Discrete Fourier Transform:

$$\frac{T}{t_1} \sum_{t_i=0}^T |\eta(t_i)|^2 = \sum_{\omega=0}^{1/t_1} \|\epsilon(j\omega)\|^2$$

As  $t_1$  is the time step and  $T$  the total simulation time,  $1/T$  is the frequency step and  $1/t_1$  the maximum frequency vector value.  $\eta$  is a zero-mean noise, when the number of samples  $N = \frac{T}{t_1}$  increases, the relation between the standard deviations  $\sigma_\eta$  and  $\sigma_\epsilon$  is  $\sigma_\epsilon = \sigma_\eta \sqrt{N}$ . On the other side,  $P_i(t)$  are typically sums of sine waves, and the amplitude of the spectral density function of  $P_i$  at modulated frequencies are directly proportional to the samples number  $N$ :  $P_i(j\omega_{mod}) = \frac{N}{2j}$ . Hence, the noise to signal ratio at the modulated frequency  $f_{mod}$  is proportional to  $\frac{1}{\sqrt{N}}$  when  $N$  increases:

$$\frac{\epsilon_i(j\omega_{mod})}{P_i(j\omega_{mod})} \propto \frac{1}{\sqrt{N}}$$

That means the longer the time-domain acquisition is, the higher the accuracy of the frequency-domain data  $P(j\omega)$  is.

#### Propagation from $P(j\omega_{mod})$ to $Q(j\omega_{mod})$

At first, the uncertainty propagation on the sound speed  $\epsilon_a$  needs to be estimated as a function of the frequency domain functions taken at the modulation frequency:

$$\frac{\epsilon_a}{a} = \frac{\epsilon_2}{2P_2} - \frac{2\epsilon_2 - \epsilon_1 - \epsilon_3}{2(2P_2 - P_1 - P_3)}$$

Using the uncertainties propagation law it is possible to calculate the standard deviation of the sound of the speed evaluation, supposing the errors  $\epsilon_1, \epsilon_2, \epsilon_3$  independent:

$$\sigma_a^2 = \frac{(\sigma_{\epsilon_1}^2 + \sigma_{\epsilon_3}^2 + \left(\frac{P_1 + P_3}{P_2}\right)^2 \sigma_{\epsilon_2}^2) 4n^2 f^2 l^2}{(4P_2^2 - (P_1 + P_3)^2) \cdot \arccos^2\left(\frac{P_1 + P_3}{2P_2}\right)}$$

Numberswise an error on the sound speed is less than 5% if the initial time-domain pressure evaluation error  $\eta(t)$  is 7% of measurement range. The expression of the error on the mass flow rate may be retrieved from the acoustic wave equation:

$$\epsilon_Q = Q \frac{\epsilon_a}{a} (ctg(kl) \cdot (kl) - 1) + \frac{S}{a} \frac{jk \frac{\epsilon_a}{a}}{\sin(kl)} (P_2 \sin(k(l+x)) \cdot (l+x) - P_1 \sin(kx)) - \frac{jS}{a} \frac{\epsilon_1 \cos(kx) - \epsilon_2 \cos(k(x+l))}{\sin(kl)}$$

To quantify the possible errors on the mass flow rate a Monte-Carlo simulation was performed with 1000 runs on the pipeline presented in the previous paragraph. For every simulation, each sensor data was artificially polluted with the white noise. The

Fig. 5 illustrates the error distribution on the mass flow rate at the modulated frequency  $Q(j\omega_{mod})$ :

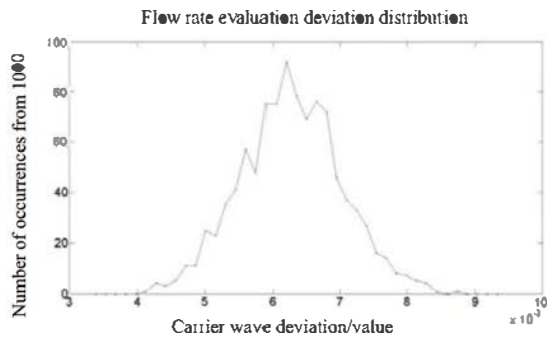


Figure 5: Mass flow rate error distribution

It can be seen at the diagram above that the estimated error may be decomposed into the systematic error of 0.6% of the flow rate fluctuation amplitude and into the random error with standard deviation of 0.1%. The variation of the input random noise standard deviation has only influence on the random error.

*Propagation to the empirical transfer function result*

The evaluation errors committed on the pressure and flow rate frequency-domain data will imply uncertainties on the final result of the transfer matrix coefficients. The exact formulation of the uncertainty propagation to the transfer matrix coefficients are presented below:

$$\frac{\epsilon_{Zm}}{Z_m} = \frac{\begin{vmatrix} Q_{e2} & \epsilon_{ps2} \\ Q_{e1} & \epsilon_{ps1} \end{vmatrix} + \begin{vmatrix} P_{s1} & \epsilon_{qe1} \\ P_{s2} & \epsilon_{qe2} \end{vmatrix}}{\begin{vmatrix} P_{s1} & Q_{e1} \\ P_{s2} & Q_{e2} \end{vmatrix}} + \frac{\begin{vmatrix} P_{e1} & \epsilon_{qe1} \\ P_{e2} & \epsilon_{qe2} \end{vmatrix} + \begin{vmatrix} Q_{e2} & \epsilon_{pe2} \\ Q_{e1} & \epsilon_{pe1} \end{vmatrix}}{\begin{vmatrix} P_{e1} & Q_{e1} \\ P_{e2} & Q_{e2} \end{vmatrix}}$$

The three other transfer matrix coefficients are expressed *mutatis mutandis* using the ETFE formulae. In the case when the user is not satisfied with the method robustness towards white noise, a user-made auto-recursive multiple input noise resistant algorithm ARMAX has been developed for this study.

**RESULTS AND DISCUSSION**

In a first series of simulations the Venturi is taken coupled with 3m ducts (with 10 nodes) at the inlet and outlet. The small number of nodes makes it impossible to apply the KDP method on this simulation. Thus, the values of pressure and mass flow rates are taken at the inlet and outlet of the Venturi tube in order to test the proposed identification methods.

The Fig. 6 and 7 show the system linearity domain. Point 1 is the evaluation of the transfer matrix using inlet mass flow rate fluctuations of 1% and 2% of amplitude, point 2 uses 2% and 3% and so on.

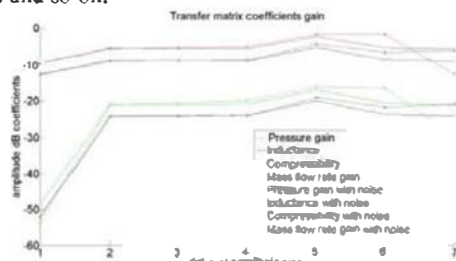


Figure 6: Gain linearity

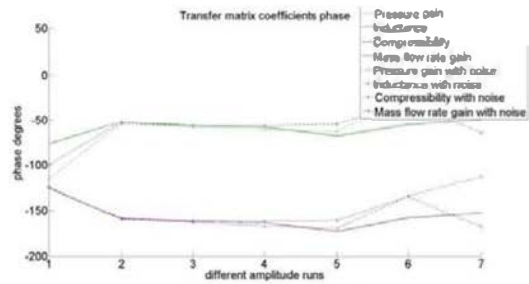


Figure 7: Phase linearity

$T_{ref}$  is 0.032s for this simulation. The tests were run with the same frequency of 5Hz. These diagrams show that for the amplitudes between 2% and 5% of flow rate modulation the gain and the phase of the system remains the same. Even with the strong input noise (7% of measurement range) the transfer matrix coefficients remain quasi-constant.

The next simulations show the Bode diagram of the frequency transfer matrix of the cavitating Venturi obtained by the empirical estimation formulae ETFE (Fig. 8 and 9)

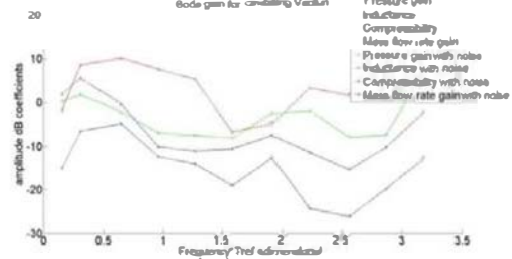


Figure 8: Bode gain for cavitating Venturi

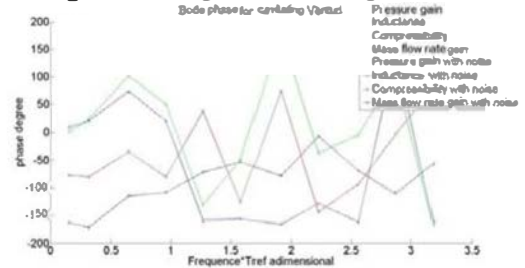


Figure 9: Bode phase for cavitating Venturi

The input noise has a less than 1dB influence on the final ETFE result. Hence the frequency per frequency method is very accurate to estimate the transfer matrix coefficients both for the gain and the phase. The drawback of this method is that the values of the transfer function are only known at the modulated frequencies. This is why it seems logical to try an identification of a transfer function for another type of input signal in order to make the identification process quicker. To perform this task, a chirp-type signal was used, because it presents a very large spectral density which is corresponding to the operator's needs. The next simulations (Fig. 10 and 11) were performed for a down-chirp signal  $\sin(\sqrt{t})$ . The spectral density of the input signal is contained between 0 and 0.2 Hz\* $T_{ref}$ . According to the graphs below, the results give more data points using only two simulations with linearly independent input vectors, however it is less accurate than frequency by frequency tests, with noise

errors reaching 5 to 10dB, even if most of the points seem very accurate. The phase errors seem however important for the inductance and compressibility, reaching 20 degrees.

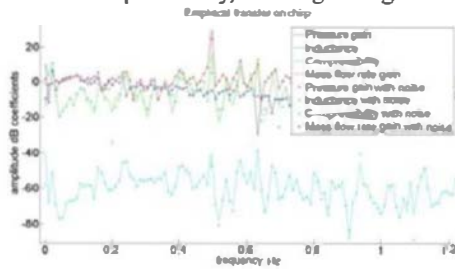


Figure 10: Bode gain for a down-chirp

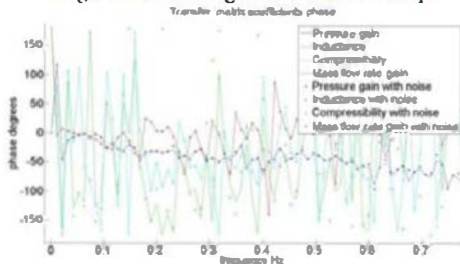


Figure 11: Bode phase for a down-chirp

In order to make the transfer matrix calculation from the ETFE input signal even more accurate and noise-proof the ARMAX (Auto-Regressive Moving Average Exogenous) identification method was implemented for this MIMO (Multiple Input Multiple Output) case [14, 15]. The chosen algorithm uses least mean squares by Kalman filter approach and forgetting factor. Only one simulation is necessary to perform the identification on the spectral domain set by the input which was chosen to be an up-chirp signal ( $\sin(t^2)$ ).

The last series of simulations of cavitating Venturi combined the mass flow rate reconstruction by KDP method, ETFE and ARMAX identification methods. Thus it is possible to evaluate the accuracy of the KDP method on the test case and the accuracy of the ARMAX identification method applied on the reconstructed pressure and flow rates, which will not be possible during experiments. The simulation was performed on the up-chirp signals with totally reflecting or totally absorbing limit conditions. The Fig. 12 and 13 allow us to compare the ETFE of the four transfer matrix coefficients on the reference inlet-outlet signals, with the ETFE on pressure and flow rate signals reconstructed by the KDP method at the inlet and the outlet and with the transfer matrix coefficients obtained by user-made auto-recursive algorithm ARMAX. The error on the sound speed reconstitution was of 1% on both the inlet and the outlet lines compared to the initially implemented value. The results show that the KDP method in this case gives up to 10dB errors for the majority of the frequencies on the transfer function identification. For the phase, the reconstructed ETFE values may present up to 90 degrees error. It has to be noticed that the zeros and poles of the system determined by the ARMAX algorithm are lying in the entire frequency domain, even if the input signal presented no power density associated to the concerned frequency. This is why sometimes the user needs to define a very high order on the system (the 30<sup>th</sup> order

was used for this simulation) which makes it difficult to link the model to any physical representation.

## CONCLUSION

In this paper the precision of the KDP method to evaluate unsteady mass flow rate and its robustness towards pressure evaluation uncertainties was evaluated. This algorithm can be used to find the sound of the speed value, and to estimate the value of the mass flow rate fluctuations, thus making it possible to perform the whole identification procedure. The frequency per frequency tests proved to be the most accurate, but also to need the biggest amount of experience data. The study of a chirp signal need much less data but is also less accurate. Finally, the KDP method seems enough precise to implement it to the experimental facility. The present work will be pursued especially to adapt the recursive algorithm part to the operator needs. The simulations presented in this paper had for purpose to develop the methodology to work with the experimental results that will come from the test facility. The tests began in April 2012.

## ACKNOWLEDGMENTS

The authors would like to express their sincere gratitude to Fabio Carvalho (LEGI) who provided his assistance for several simulations with the IZ code, as well as to A. Pintiau, A. Kemilis, J. Toutin (Snecma) for their help with KDP method of the unsteady flow measurement, to J.J. Martinez (Gipsa-lab) for the explanation of the auto-recursive identification methods, and finally to O. Brugiere (LEGI) for his advice about the uncertainties propagation. We would especially like to thank the Centre National d'Etudes Spatiales for the IZ simulation code.

## NOMENCLATURE

P – fluid static pressure, frequency domain  
 Q – mass flow rate, frequency domain  
 Z – impedance  
 p – fluid static pressure, time domain  
 u – fluid velocity, time domain  
 $C_f = \lambda/4$  – friction coefficients  
 a – speed of sound in the pipe  
 c – speed of sound in the water  
 D – pipe diameter  
 e – pipe wall thickness  
 E – pipe material Young modulus  
 S – pipe section  
 x, dx – coordinate, space step  
 t, dt – time, time step  
 g – gravity  
 k – wavenumber  
 l – distance between pressure evaluations  
 f – frequency  
 T – total simulation time  
 N – number of samples  
**Greek letters**  
 ρ – fluid density  
 ω – pulsation

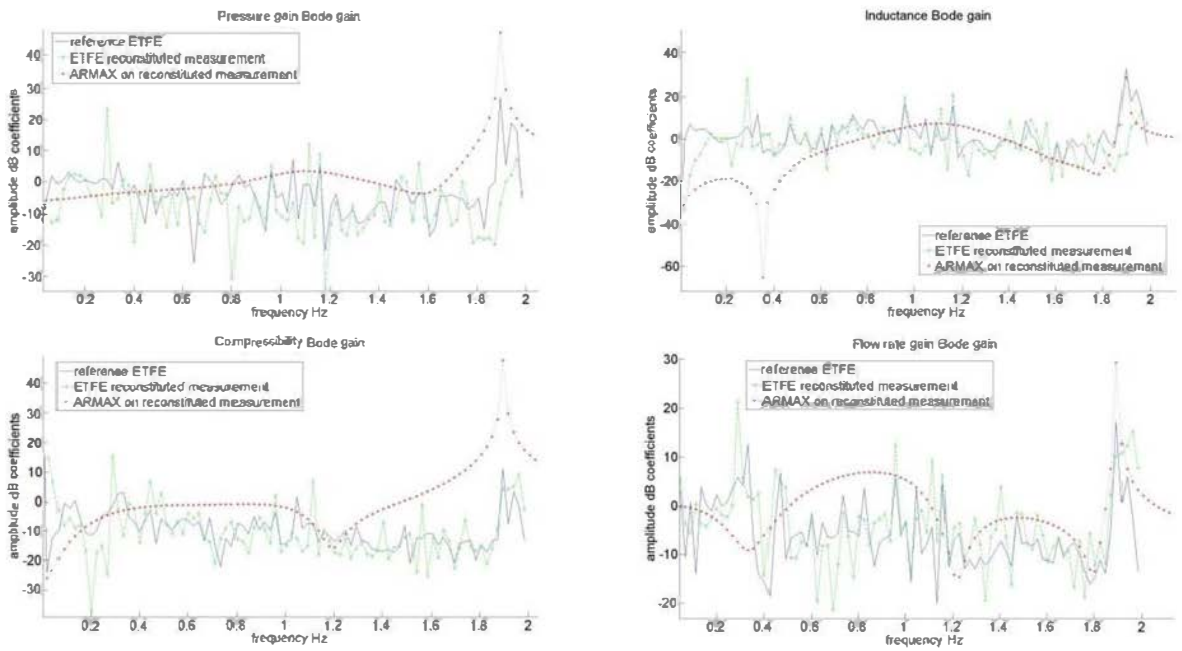


Figure 12: Bode gain diagrams

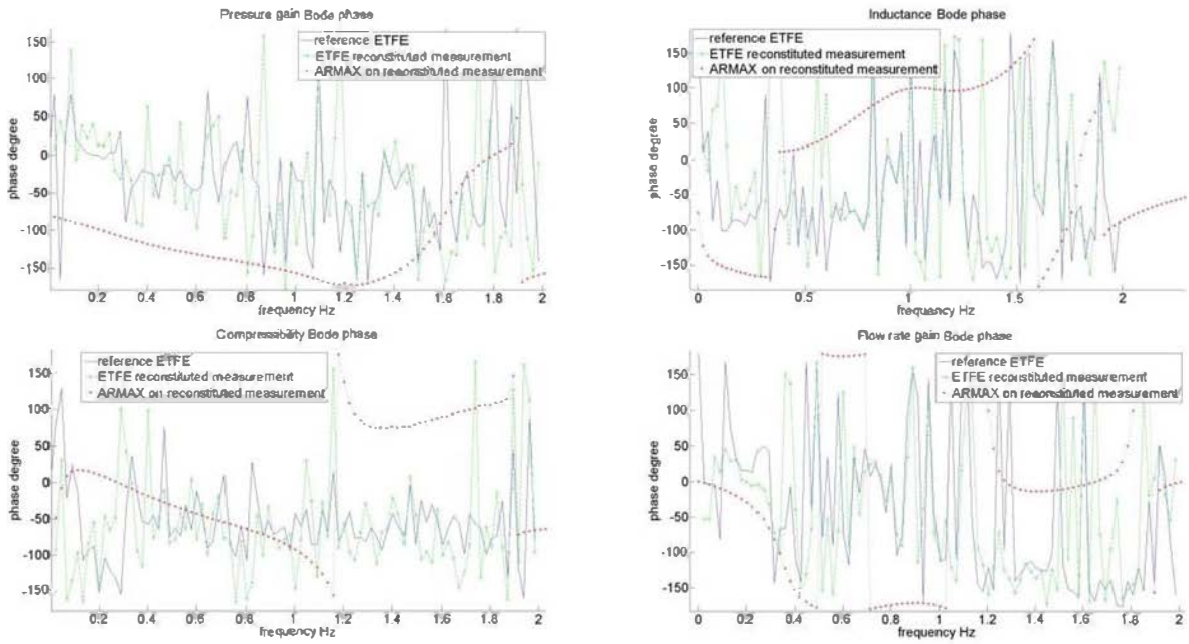


Figure 13: Bode phase diagrams

$\sigma$  – standard deviation  
 $\eta$  – time domain noise on pressure signal  
 $\epsilon$  - frequency domain noise on pressure signal  
**Superscript**  
 ~ - fluctuating quantities  
**Subscripts**  
 m – pressure gain

L – inductance  
 C – compressibility  
 M – Mass flow gain  
 i – inner  
 e – inlet  
 s – outlet  
 1, 2, 3 – pressure data nodes

$\mathbf{l}, \mathbf{2}$  – non-collinear vectors  
 mod – modulated  
 $\mathbf{a}$  – speed of sound  
 $\mathbf{Q}$  – mass flow rate  
 $P$  – pressure  
 $Z$  – impedance  
 $\epsilon$  – frequency domain noise on pressure signal  
 ref – reference

## REFERENCES

- [1] Ren H., Ren G., Rong K., Ma D., Zhang J., A non-linear model of the simulation of the pogo vibrations in liquid rockets, *Structure and environment engineering*, vol. 33 N°3, 2006 (in Chinese)
- [2] T. Shimura, K. Kamijo, Cavitation induced flow vibration of liquid oxygen pumps for rockets, *JSME N°87-1318B* (in Japanese)
- [3] C.E. Brennen, A.J. Acosta, Dynamic transfer function for a cavitating inducer, *Journal of Fluids engineering* vol.98, 1976
- [4] V.V. Pilipenko, S.I. Dolgoplov, N.V. Horyak, A.D. Nikolaev, Mathematical modelling of longitudinal oscillations of liquid propellant rocket during bipartial instability of the dynamic system LPRE – rocket structure, *Airspace Technics and Technology*, N°10 (57), 2008 (in Russian)
- [5] J.F. Lauro, A. Boyer, Transmission matrix and hydroacoustic sources of a centrifugal pump at very low load, *La Houille Blanche*, N°374, 1998 (in French)
- [6] J.J. Dordain, M. Marchetti, Transfer matrices of hydraulic systems. Theoretical and experimental study, *Airspace Research* N°1-1974 (in French)
- [7] Coutier-Delgosha O., Reboud J-L., Delannoy Y. (2003), "Numerical simulation of the unsteady behaviour of cavitating flows", *Int. J. for Numerical Meth. In fluids*, Vol. 42, pp. 527-548.
- [8] NG, S.L., Brennen, C., Experiments on the dynamic behavior of cavitating pumps, *Journal of Fluids Engineering*, vol.100, 1978
- [9] Lefebvre, P.J., Durgin, W.W., A transient electromagnetic flowmeter and calibration facility, *Journal of Fluids Engineering* 12/vol.112, 1990
- [10] Choi, J.-S., McLaughlin, D.K., Thompson, D.E., Experiments on the unsteady field and noise generation in a centrifugal pump impeller, *Journal of sound and vibration* 263 (2003) pp. 493-516
- [11] Elkins, C.J., Alley, M.T., Magnetic resonance velocimetry : applications of magnetic resonance imaging in the measurement of fluid motion, *Experiments in Fluids*, N°43, 2007
- [12] Katys, G.P., Methods and apparatus to measure parameters of unsteady thermal processes, ed. *Mashgiz*, Moscow, 1959, part 4, ch.3, (in Russian)
- [13] Kashima, A., Lee, P.J., Nokes, R., Numerical errors in discharge measurements using the KDP method, *Journal of hydraulic research*, iFirst 2011, pp 1-7, DOI:10.1080/00221686.2011.638211
- [14] Fassois, S.D., MIMO LMS-ARMAX identification of vibrating structures – part I: the method, *Mechanical systems and signal processing* (2001) 14(4), pp. 723-735
- [15] Moore, S.M., Lai, J.C.S., Shankar, K., ARMAX modal parameter identification in the presence of unmeasured excitation – I: Theoretical background, *Mechanical systems and signal processing* 21 (2007) pp. 1601-1615
- [16] Priel, M., Incertitudes de mesure et tolerances, *Dossier Techniques de l'Ingénieur*, r285, 1999 (in French)
- [17] S. Rubin, "An interpretation of transfer function data for a cavitating pump," in *Proceedings of the 40th AIAA Joint Propulsion Conference*, Fort Lauderdale, Fla, USA, 2004, AIAA-2004-4025.
- [18] Thompson K.W. (1987), "Time dependent boundary conditions for hyperbolic systems", *Journal of Computational Physics*, Vol. 68, pp. 1-24 and (1990), "Time dependent boundary conditions for hyperbolic systems, Part II", *Journal of Computational Physics*, Vol. 89, pp. 439-461.
- [19] F Longatte, J L Kueny (1999), "Analysis of rotor-stator-circuit interactions in a centrifugal pump", *Proceedings of the 3rd ASMEJSME Joint Fluids Engineering Conference*